prepared for the
National Institutes of Health
National Institute of Neurological Disorders and Stroke
Neural Prosthesis Program
Bethesda, Maryland 20892

ELECTRODES FOR FUNCTIONAL ELECTRICAL STIMULATION

Contract #NO1-NS-6-2346

Quarterly Progress Report #5
January 1, 1998 - March 31, 1998

Principal Investigator
J. Thomas Mortimer, Ph.D.

Applied Neural Control Laboratory
Department of Biomedical Engineering
Case Western Reserve University
Cleveland, OH USA

THIS QPR IS BEING SENT TO YOU BEFORE IT HAS BEEN REVIEWED BY THE STAFF OF THE NEURAL PROSTHESIS PROGRAM.

TABLE OF CONTENTS

SECTION A. CLINICAL COLLABORATION

We met with our clinical collaborators in quarter 5. The focus of the meeting was on human applications and animal testing associated with the electrode. Three candidate systems emerged for further consideration. These systems are a lower extremity system, an upper arm/shoulder application, and a blocking application for spasticity and phantom limb pain. Of these three candidates, the lower extremity system appeared to be the earliest target, but plans are still not firm. A major point discussed in the meeting was the animal testing. It was felt by the collaborators that the FDA would prefer that animal testing be done on the entire system that would be used in a human for a particular application, rather than a collection of studies on separate elements of the implanted device, if at all possible. Because no applications have yet been defined, this leaves the animal testing currently being done with the same general focus it has taken in the past, which qualifies as testing for a more generic application of cuff electrodes. Another point of uncertainty was the connector for the system. It was thought by the collaborators that the connector might need to be application specific and at this time we have only one candidate connector, a four-pin connector.

Meetings will continue to explore applications for the cuff electrode.

SECTION B. DESIGN AND FABRICATION OF ELECTRODES, LEADS AND CONNECTORS

B.2.1.2: Polymer-Metal Foil-Polymer (PMP) Cuff Electrodes

The polymer-metal foil-polymer (PMP) electrode is a novel design that attempts to improve the mechanical reliability and ease the manufacturing process of spiral nerve cuff electrodes. The electrode design uses laser micromachining technology to fabricate an electrode pattern in a polymer-metal foil laminate. During this reporting period, a second version of the electrode pattern has been designed and is presently being implemented.

Previous Work

In earlier quarters, the PMP2 electrode was developed and the first fabrication attempt was made on two electrodes. In QPR#4, we illustrated the electrodes after the first laser pass and the first lamination. Careful study with electron microscopy proved the precision of the laser machining.

Current Work

The fabrication process was continued on the PMP2 electrodes. Step 3 of the process, the laser cutting of the paths, weld sites, and excising, was performed successfully. The results from this step are seen in the figures below.

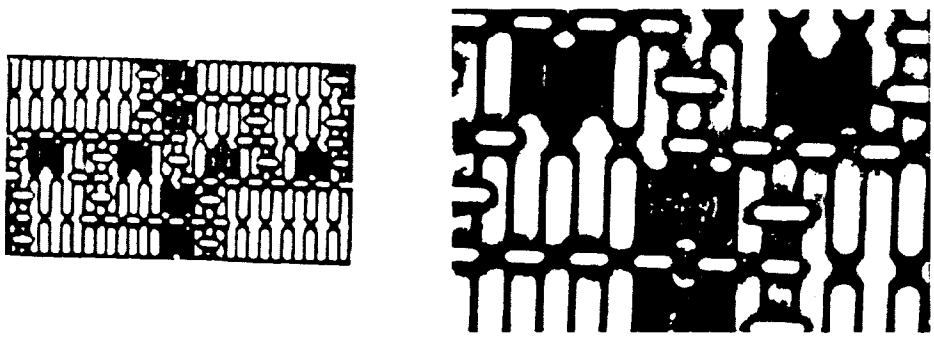

Figure B.1: The pictures displayed above show that the structure of the electrode has been preserved after the 2nd laser pass. The precision of the laser cutting on both the platinum and the lamination can also be seen. The picture on the right is a magnified view of a weld site where the contact window was cut using the laser.

With step 3 complete, closed helix leads were made and welded to the weld sites. This welding proved to be very difficult due to our inability to cut the wires to the precise lengths required for perfect alignment in the lead section. Because the four wires come out of the helix parallel to one another, and because they are to be welded to sites that are vertically aligned,

wires must at some points overlap. It is the overlapping of these wires and the slack necessary to do so that is unpredictable. Because of this fact, one of the electrodes was tilted with respect to the lead assembly. This produced a cuff that was twisted off of the desired 90° exit line.

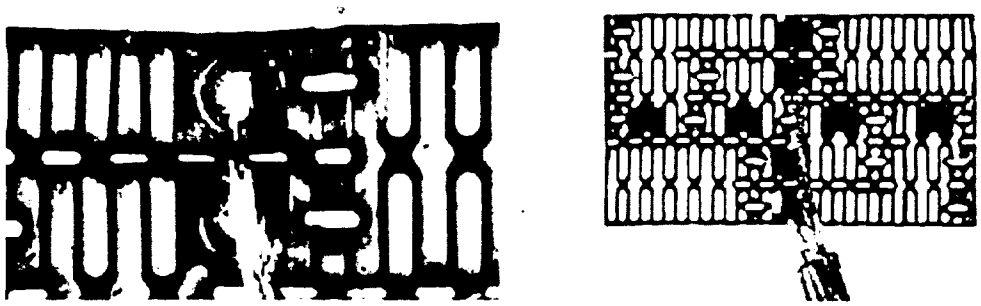

Figure B.2: The above pictures allow us to observe the close proximity for the lead wires within the weld site. Revealed in the picture on the left is the quality of the weld and the importance of the amount insulation removed from the lead. If too much insulation is removed, a lead could contact another site or path on the electrode. It is seen in the picture on the right that due to the vertical alignment of the weld sites, the lead assembly is forced to angle to one side. This error occurred because of the uncertainty in cutting the lengths of the lead wires.

Step 5, the final cuff lamination, was performed on both electrodes from Figure B.2. This step revealed some problems in the fabrication process. The platinum structure in one of the electrodes tore during the pressing. It was later discovered that the elastomer used in this step was over 6 months older than its shelf life. The elastomer becomes more viscous with age. So, with this more viscous elastomer between the openings of the electrode, squeezing the mold assembly too quickly may generate pressures within the elements of the P-M-P structure that are high enough to break the electrode apart.

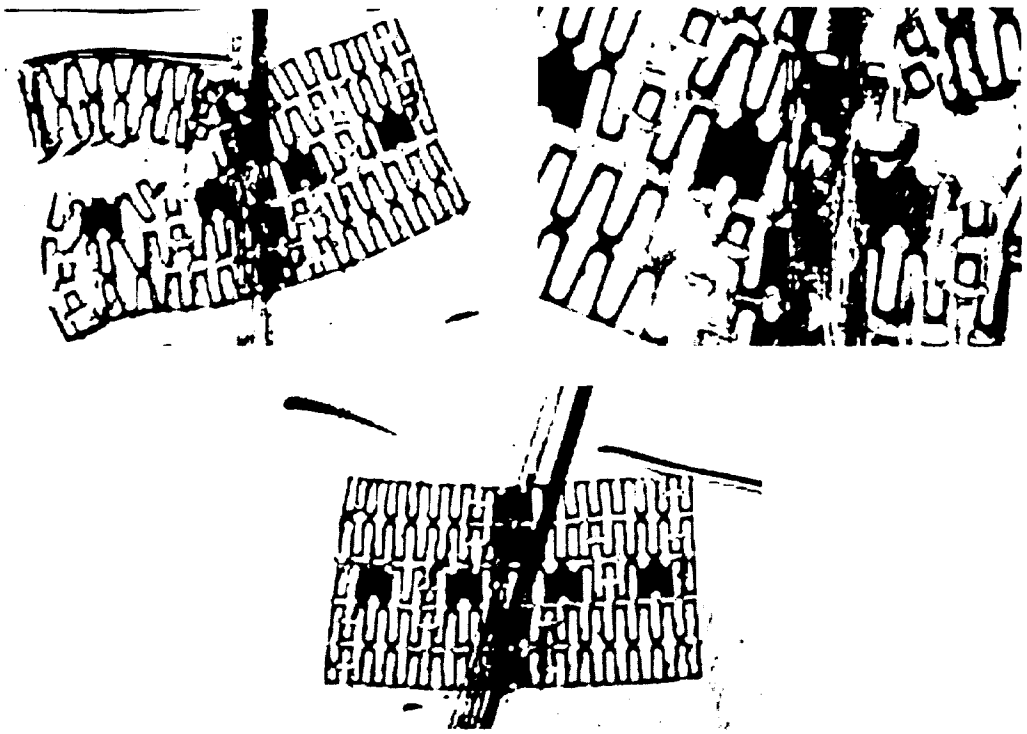

Figure B.3: Looking at the top two pictures one can see that tearing took place in one of the electrodes. Not only does this occurrence give insight into the problem in the fabrication process, but it also highlights where mechanical failure is most likely to occur. The bottom picture is of the electrode that remained in tact. Unfortunately, this electrode is angled with respect to the lead and the cuff. This makes it undesirable for implant.

It was also found that the elastomer did not distribute evenly between the plates. This caused one of the electrodes to have a very thin, tight cuff, and the other electrode to have a thick, large cuff. It is believed that the thick elastomer was partly responsible for this. Another contributor was probably the lead assembly. The assembly for this electrode has a larger diameter than leads used in the past. Because of its size, it did not entirely fit into the groove in the electrode plates. Instead, it was raised above the surface of the plates, which may have restricted flow of the elastomer. Because of the damage of the cuffs, step 6, the opening of the stimulation sites, was not pursued.

Despite the damage caused in step 5 of the process, it was felt that the PMP2 electrode fabrication process could be corrected. Fabrication of a new batch of electrodes was therefore attempted. Four new stainless steel frames were made for use in the fabrication process. New AutoCAD files were also created to support the range of sizes desired. Specifically, these sizes were 2.55, 2.8, 3.0, 3.2, and 3.45mm cuffs. Five pieces of platinum foil were then placed in the five frames and the first laser pass took place. The laser cut ten electrodes; 2 each of 5 different sizes. This step was successful and pictures documenting this step are shown in Figure B.4.

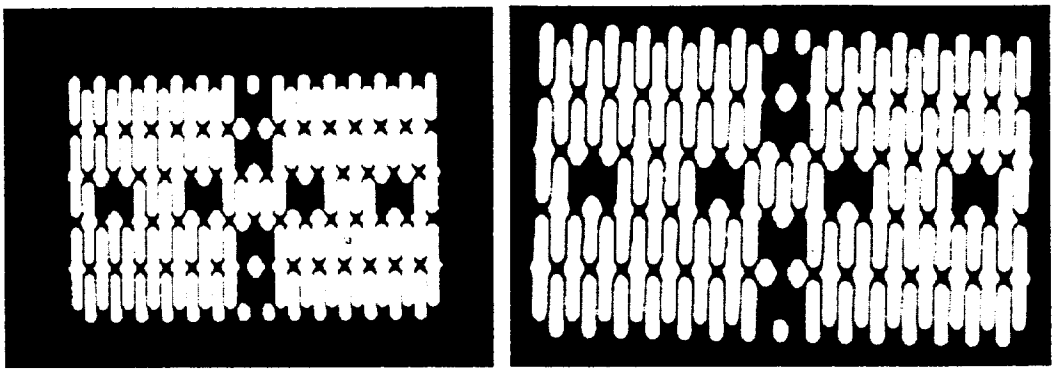

Figure B.4: It can be deduced from these two pictures that the 1st laser machining pass was successful. The structures of all ten electrodes were accurate and precise according to what could be seen with the microscope.

With step 1 complete, the platinum structures were then laminated. The first two pieces of platinum laminated were difficult to remove from the plates after lamination. This caused some geometrical damage to the electrodes. The lamination process was then improved by adding a backing of mylar to the lamination configuration so that the laminated electrode could be more easily removed. The next three laminations were then successful. Pictures highlighting the damage that occurred on the smaller electrodes and the success of the larger electrodes are shown in Figure B.5.

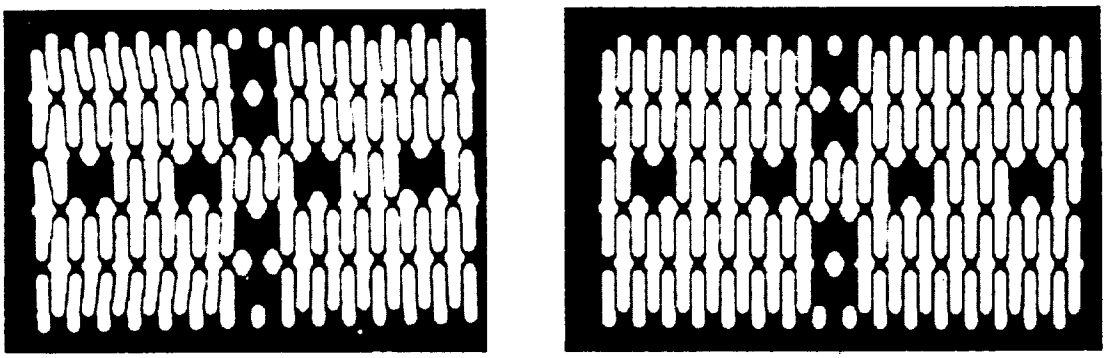

Figure B.5: The picture on the left is a picture of the laminated PMP2 structure for a 2.8 mm cuff electrode. Geometrical damage can be seen on the left side of the picture. This can be compared to the picture in Figure B.4 which shows the metal component of the PMP2 structure before lamination. The picture on the right is of the laminated structure of a 3.2mm cuff electrode. This electrode looks to have retained its intended structure. This is due to an improvement in the lamination process.

It is possible that we still may be able to use the laminated 2.8mm structure since the distortion was outside of the conductive pathways. Step 3 was completed successfully, however, much of

the laser machining on the damaged electrodes had to take place manually due to the geometrical changes in the damaged electrodes. The results of step 3 are shown in the pictures below.

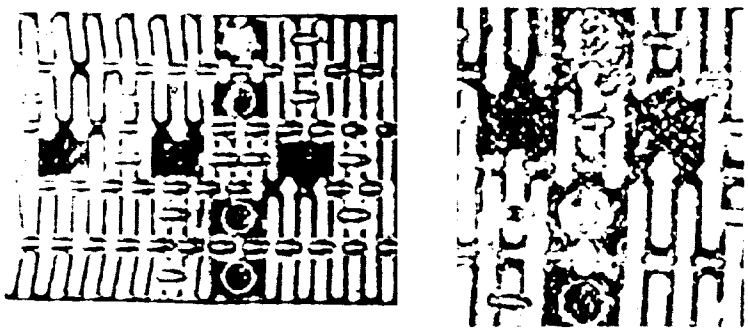

Figure B.6: It can be seen in the picture on the left that the geometrical structure of the electrode was deformed during the lamination process. These pictures also show that the laser machining was still successful on this electrode. The path cuts and weld sites are where they need to be despite the variance in the geometry from the AutoCAD file used in the laser machining process. The picture on the right, however, does highlight some difficulty in the removal of the weld pads. The cuts in the lamination do not appear as smooth as what is normally seen. This is due to a variance in the lamination thickness. This is not expected to in any way effect the function of the electrode.

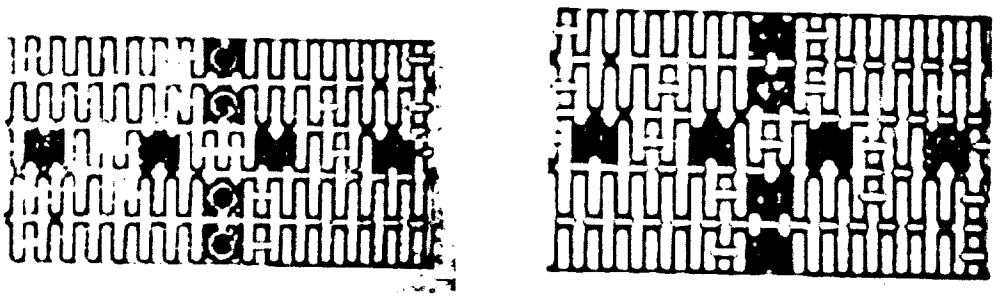

Figure B.7: The pictures in this figure were taken of two different sized electrodes after the 2nd laser pass. These electrodes have not been damaged in the process and the 2nd laser pass went as expected.

Future Work

With step 3 complete, decisions will be made as to whether or not some of the damaged electrodes will continue on with the fabrication process or be terminated. The remaining electrodes, however, will continue through the fabrication process and, if completely successful, will be used for the animal testing. Work will be done to solidify a detailed fabrication protocol. Improvements to the fabrication process will continue.

B.2.2: Lead Designs

Previous Work

Testing began in Quarter 2 on the silicone rubber overcoated wire, which was obtained from PI Medical and Specialty Silicone Fabricators (SSF). This testing involved winding the wires around madrels, removing the mandrels, and looking at the resulting helixes with electron microscopy. These tests were continued in Quarter 5.

Current Work

The first question we faced was to determine which of the SSF samples of wire were with the fluoropolymer corona etched prior to silicone rubber coating and which ones were not. This information had been lost upon delivery of the material. Technical representatives at Temp-Flex, the company that performed the corona etching, told us that corona etching allows for the material, fluoropolymer PFA, to be written on. Normally, the fluoropolymer insulation on the wire cannot be written on. The Temp-Flex representatives claimed that this property of corona etching was permanent.

This information was tested by taking samples from the two different spools of silicone rubber overcoated wire from SSF. These samples were soaked in Freon, which made the silicone rubber swell. The silicone rubber jacket was then removed from the insulated wire. The remaining sample was then marked with a permanent marker. It was found that on one set of samples the ink beaded and could be wiped off. On the other set of samples, the ink set and became a permanent mark. It was therefore determined that the spool used to create the sample upon which the ink beaded, was corona etched.

The person we spoke with at Temp-Flex also told us that other customers had reported that while corona etching causes a roughening of the surface, which increases the material's adhesive properties, it has been found that the added adhesion only lasts for approximately 30 days. Because increased adhesive properties are the desired effect for this particular application, it was decided that corona etching would not be beneficial in the long term for the silicone rubber overcoated wire.

With many process questions answered, the performance of the wires was yet to be determined. In order to test this, samples from PI Medical, and Specialty Silicone Fabricators corona and non-corona etched wire were wound around mandrels of sizes 5, 7, and 9 mil. These samples were then studied, with the scanning electron microscope, with both the mandrel in the helix, and the mandrel removed. The winding was done using a pitch of 10° and a tension of 30g. The mandrels were removed by soaking the helix in the surfactant LiquiNox. The following figures illustrate the results of these silicone rubber overcoated wire samples wound into helical form.

Figure B.8: The two pictures seen above are wire samples from PI Medical. The picture on the left is wire wound around a 9 mil mandrel, while the picture on the right illustrates the wire after the mandrel was removed. It can be seen that the Siliblate coating the wire came off during the winding process. In fact, it often came off by touching it. For the parts where the Siliblate did not come off, the picture on the right shows that the Siliblate often grossly deformed.

Figure B.9: The two pictures shown here illustrate the results we noted with the SSF wire that was corona-etched. These wires were also wound around a 9 mil mandrel. An improvement in the durability of the wire compared to the wire coated with Siliblate can be seen. This wire was coated with NuSil's MED 4750. The only damage that appeared on this wire is the wrinkle seen in the right hand picture. This could have been caused by a sharp edge on the mandrel. As it was removed it could have caught in that spot.

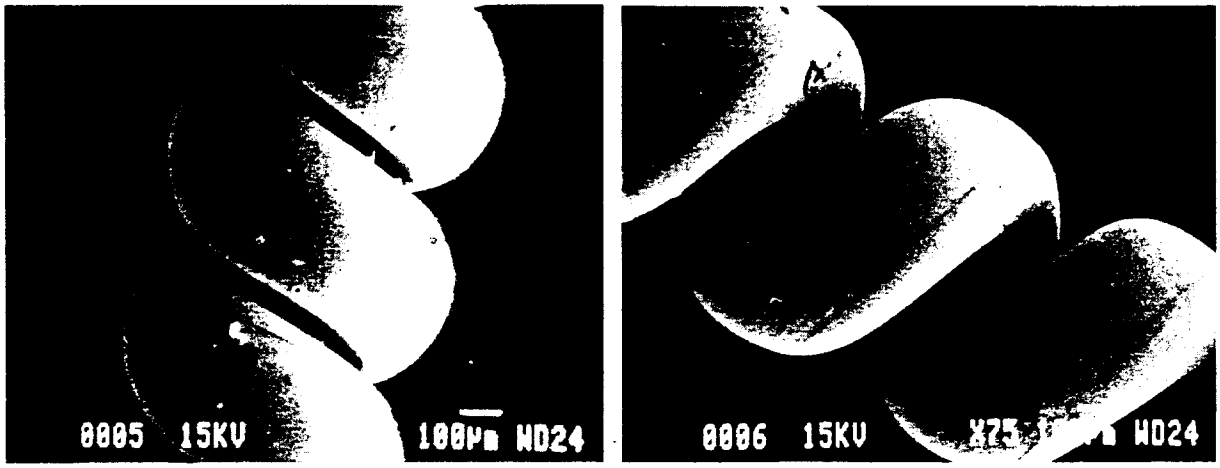

Figure B.10: The two pictures seen here are of the SSF wire without corona etching. This wire showed the same durability as the previous samples. No deformations were found on the wires with or without the 9 mil mandrel. Under electron microscopy, the wire appears smooth and with very few natural defects.

It can be seen from the pictures in Figure B.10 that both Specialty Silicone Fabricators' products have satisfactory properties in the helical form. The fact there is no obvious difference in the result of the corona and non-corona etched wire supports the statement that corona etching loses its adhesive properties after 30 days. This particular wire batch is almost a year old.

The results of the winding further support a decision to use of the Specialty Silicone Fabricator non-corona etched silicone rubber overcoated wire because 5,7, and 9 mil mandrels are all smaller than the mandrel size which would be optimally used. The optimal size mandrel should result in an even smoother looking helix without deformation of the silicone rubber in any way.

Future Work

Future studies will include winding the Specialty Silicone Fabricator non-corona etched wire around mandrels ranging in size from 9 to 15 mil. These helices will then be studied using electron microscopy. It is expected that this will reveal the optimal mandrel size and winding specifications so that this wire can be used in future applications.

In earlier quarters, 2 different electrode designs (the PMP and the FWF), were pursued and a single electrode of each were fabricated. The results from this initial production were encouraging and demonstrated the feasibility of laser machining technology for electrode fabrication. While deficiencies in both designs and their manufacturing techniques were identified, so too were their strengths. A third electrode design, which we have designated as the PMP2 electrode, is being pursued. This electrode incorporates the advantages of the previous designs while avoiding the observed deficiencies.

B.2.4.2: Weld Strength

Before welding could begin on this PMP electrode, a welding method had to be devised which would allow for current to pass through the small window opening in the lamination for the weld to occur. This involved building a new welding table that allows for a point contact on both the top and bottom of the electrode. The lamination prohibits using the flat copper table since current does not pass through the silicone rubber, and the lamination prevents platinum from touching the table. A schematic of the new weld table is shown below.

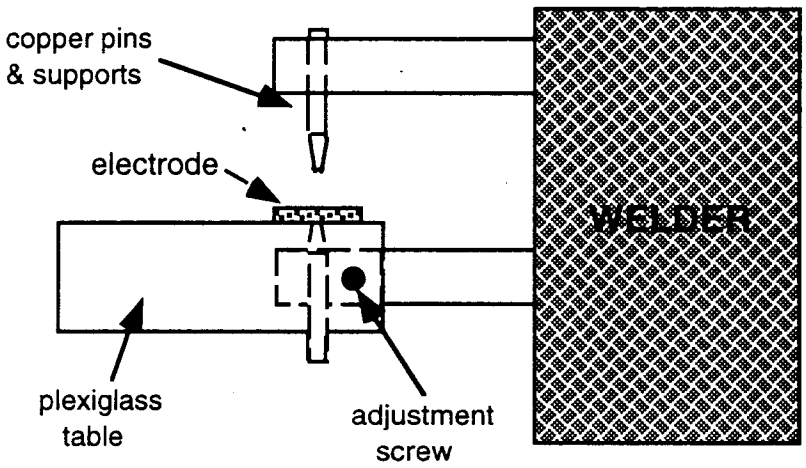

Figure B.11: This figure is a simple model of the weld table that was built to weld on the PMP2 electrode. The pin from the bottom is embedded in the table with a setscrew from the other side. It can also be adjusted for height so that the pin just touches the platinum which is approximately 100 microns from the surface of the table due to the lamination. This weld process should be able to weld on any future electrodes created because of its adjustability.

With this method developed, an effort was made to determine the best weld settings for this electrode. A range of currents from 0.6mA to 1.2mA and forces ranging from 30 to 50 ounces were used to determine the strongest weld. Wires were welded using the different combinations and then tensile tested. It was found that the strongest range on welds was around 0.8 and 1.0mA with forces at 30, 40, and 50 ounces. More samples were made within this narrowed range and tensile tests were again performed. This testing revealed that 1.0mA and 50 ounces result in the strongest weld. At this setting the wire reaches its ultimate tensile strength before the weld.

Future Work

With the best settings determined, it was felt that the samples used in the weld strength testing needed to be as close to the electrode sites as possible. Samples of laminated platinum will have multiple windows removed by the laser so that testing may take place. Welds will be tensile tested to failure after aging and press curing. These tests will offer information on the

strength of these welds after they have endured the electrode fabrication process and after implantation in the body. Results of this testing will be presented in QPR #6.

B.2.4.3: Contact Window

Previous methods used to fabricate employed a metal cannula to open "windows" in the silicone rubber surface of the PMP structure. Microscopic examination of the platinum underlying the "window" revealed that the foil was often damaged by this procedure. It was proposed in the contract proposal that this procedure be studied and modified to ensure that an accurate and non-damaging "window" was made.

In developing this PMP electrode, it was discovered that the laser used to cut the platinum foil could also be used to remove the silicone rubber on the contact sites. This has been done, and found to be a much more precise method. The contact windows are always cut to 0.5mm in diameter, and the laser never damages the foil. The only possibility for damage from this procedure is the process of removing the silicone rubber pad after the laser cut is made. Currently, these pads are removed with forceps. This method has the possibility of scratching the platinum with the forceps tip. These scratches have not been found to cause any functional damage to the electrode. However, this process will continue to be observed and improvement will continue to be an impetus.

SECTION C. IN VIVO EVALUATION OF ELECTRODES

C.I.2.1.2: Electrode Selectivity: Sub-Fascicular

Abstract

Experiments were performed to effect selective activation of motor fibers served by subdivisions of the tibial and common peroneal nerves through a multicontact self-sizing spiral cuff electrode positioned on the sciatic nerve of a cat. Torque output for each subdivision of the tibial and common peroneal nerves were found using multi-contact electrodes placed directly on each branch. Applying anodic and cathodic field steering techniques from an electrode placed around the sciatic nerve, selective activation of subdivisions of the tibial and common peroneal nerves were found to be possible in two of four trials.

Purpose

The purpose of this project is to demonstrate selective activation, from threshold to maximum, of a population of motor nerves serving a single muscle and contained within a fascicle containing nerve fibers serving several muscles. The model system studied uses a four contact self-sizing cuff electrode placed on the cat sciatic nerve. This nerve contains four major branches that serve the 13 muscles controlling the torque produced about the ankle. The focus of the studies reported here was to first document the torque profiles for the separate and distinct motor axon populations within the common peroneal and/or tibial nerves. The next objective was to demonstrate that these distinct motor axon populations, serving separate muscles, could be activated separately and independently with "field steering" applied from the four contact electrodes positioned around the sciatic nerve.

Background

Data collected, during experiments carried out over the past four years, suggest that selective and independent activation of a subdivision of the tibial or common peroneal nerve is possible from a four contact cuff electrode placed on the sciatic nerve. In Figure C.1 is shown the torque recorded when stimulation was applied from two separate electrodes. In each of the two cases, the torque trajectory follows two different pathways to the same maximum torque. The tibial branch electrode appears to activate the motor axons serving the FHL/FDL/TP first, followed by the motor axons serving the PLN. Whereas stimulation applied to a contact on the sciatic nerve appears to activate the motor axons serving the PLN first followed by the motor axons serving the FHL/FDL/TP. Refer to Figure C.2 for torque trajectories characteristic of FHL/FDL/TP and PLN.

Data presented in Figure C.2 comes from Lawrence [1993] for the cat ankle positioned at 90° flexion. Each of the four solid vector lines is the summation of the individual output torque produced by each muscle within each of the four fascicles. Both the tibial and common peroneal fascicles were further broken down to show the summation of muscles that have anatomically similar branching, shown with dotted vector lines. Based on these muscular sub-groupings, the tibial fascicle is composed of two sub-populations of axons that innervate muscles that produce two different torque vectors. The plantaris produces primarily plantar flexion while the

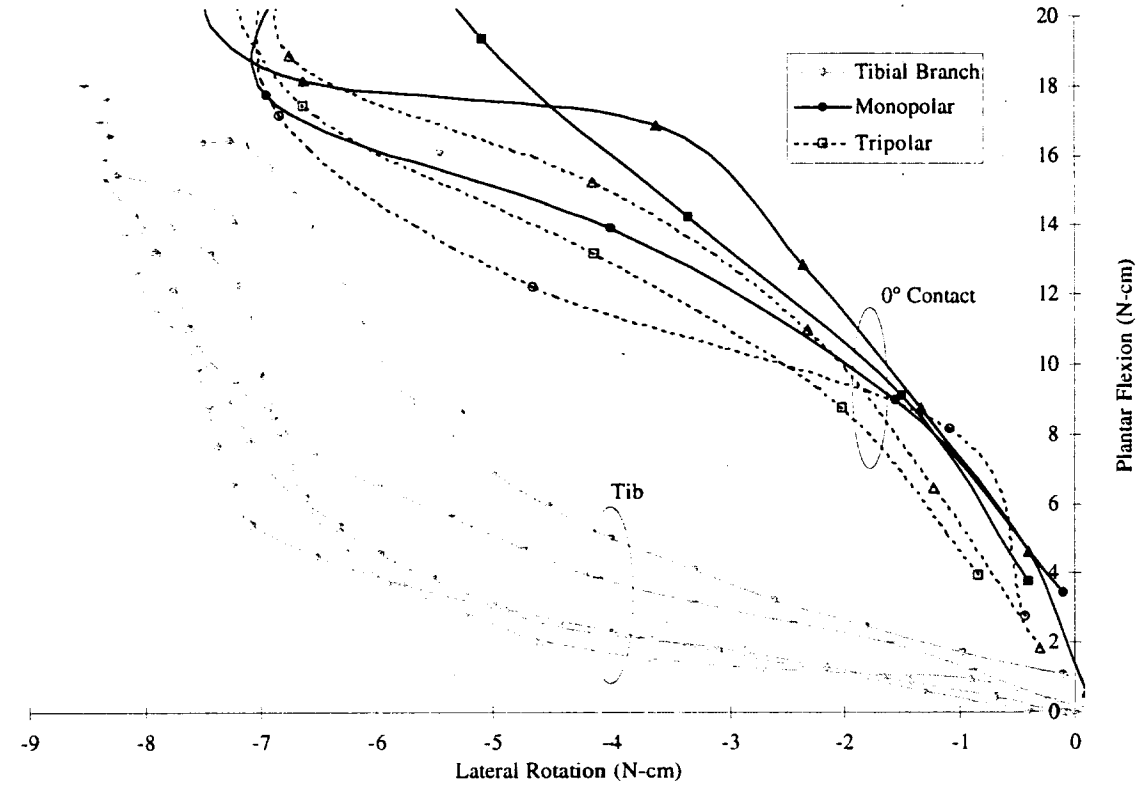

Figure C.1 - An example of how the tibial branch electrode recruited activation to produce medial rotation followed by plantar flexion while the nerve cuff electrode recruited activation to produce the plantar flexion first followed by medial rotation.

combination of the flexor hallucis and digitorum longus and the tibialis posterior produce medial rotation with some plantar flexion. The difference in the order of recruitment produced by the tibial nerve electrode and the 0° contact was attributed to spatial selectivity. This is because no temporal differences are imposed and differences in axon size would cause both stimulation sites to recruit the same large fibers first and small fibers second. Spatial selectivity supports previous work by indicating that grouping of axons within the nerve is maintained. [Brushart 1991, Hallin 1990, Schady et al. 1983] It further indicates that inside of the perineurial scattering barrier of individual fascicles, the excitatory field affects one spatial region within that fascicle before the rest of the fascicle.

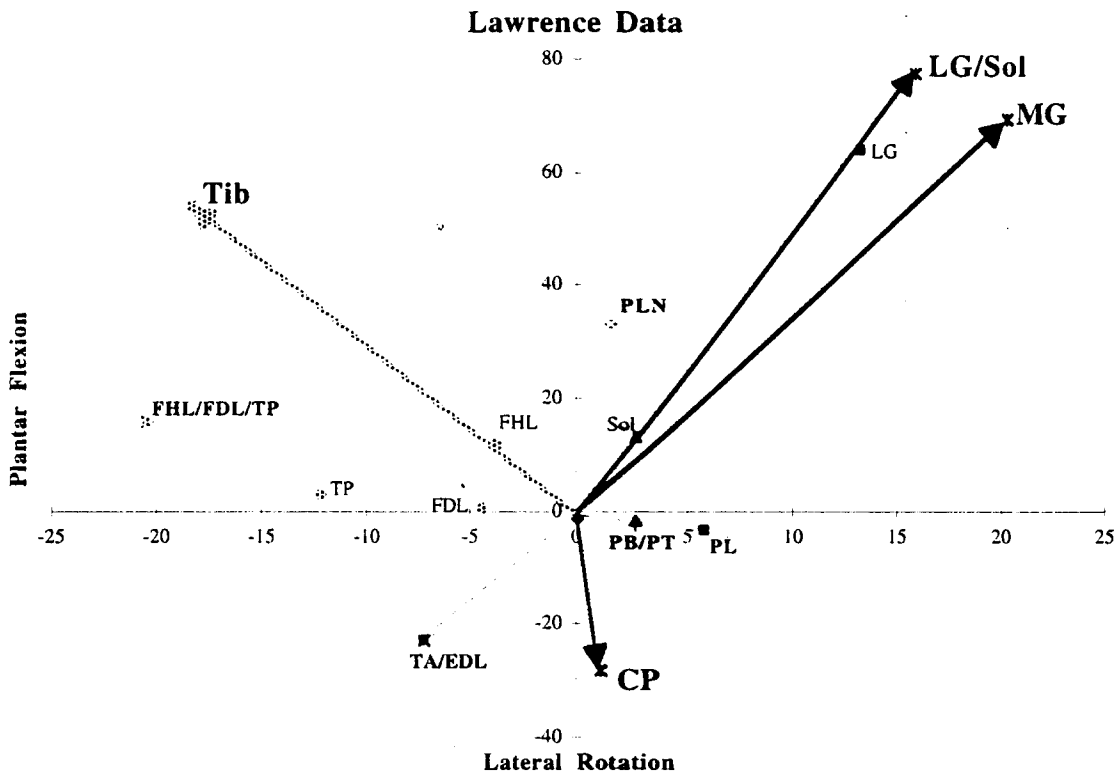

Figure C.2 - Data from Lawrence [1993] of the torque output of each of the muscles controlling the ankle joint of a cat. Muscles innervated by the same fascicle within the sciatic nerve are grouped together with the bold labels and bold vector lines indicating the output torque direction of the sum of the individual muscles. The dotted vector lines are the sum of the output torque of muscles with axon populations that are geometrically close in the sciatic nerve.

Progress

Data were recorded and processed from four experiments. Details of the methods used are described by Grill et al. (1996). Briefly, self-sizing spiral cuff electrodes were placed on the sciatic nerve of adult cats and its corresponding four branches. The ankle torque was measured in response to electrical stimuli applied to the radial spaced contacts in each cuff. The focus of our efforts during this project was to demonstrate that field steering techniques could be used to activate, selectively and controllably, distinct motor axon populations. These populations serve separate muscles and are located within a single fascicle contained within a nerve trunk that serves many muscles. In these experiments, our first objective was to identify a fascicle (either the common peroneal or the tibial) whose branch could be stimulated to produce torque output indicative of separate axon populations activated in two or more different orders. We then proceeded to impose field steering and pre-pulse techniques to the appropriate contact, that best activates the corresponding fascicle, to achieve separate and independent activation of the identified axon populations.

Experiments #1&2: Cat #315 & Cat #363

The first two experiments were reported in the previous reporting period, NIH QPR#4. In one animal, cat #315, an increased separation of activation of populations within a single fascicle was achieved. The results of a second animal, cat #363 were inconclusive due to a lack of torque separation produced by the individual electrodes that were placed directly on the individual fascicles. In both cases, only one order of activation of the individual populations was achieved.

Experiment #3: Cat #367

In the third experiment, cat #367, sub-fascicular separation was achieved using the electrodes on the common peroneal nerve, Figure C.3. Individual contacts on the common peroneal nerve were found to produce torque output ranging from primarily lateral rotation to mostly dorsiflexion with a small amount of medial rotation. None of the individual contacts activated the tibialis anterior/extensor digitorum longus, TA/EDL, portion of the common peroneal first. The thick dash-dot lines were used to approximate the TA/EDL torque output produced. This was done by using the dash-dot line on the right side to approximate the size and angle of the torque vector and then the copy on the left translates the magnitude and direction to the origin of the axis. Stimulation from the 270° position was able to achieve the common peroneal nerve, shown in Figure C.3. Based on the direction of the torque output the 270° contact first activated the TA/EDL portion of the common peroneal. The introduction of anodic steering current from the 0° position to the 270° position was found to increase the magnitude of torque output, in the direction of the TA/EDL, before spillover. We believe the addition of the steering current caused the additional sub-fascicular separation. Under the time constraints of the experiment, we were unable to demonstrate selective activation of the motor component of CP.

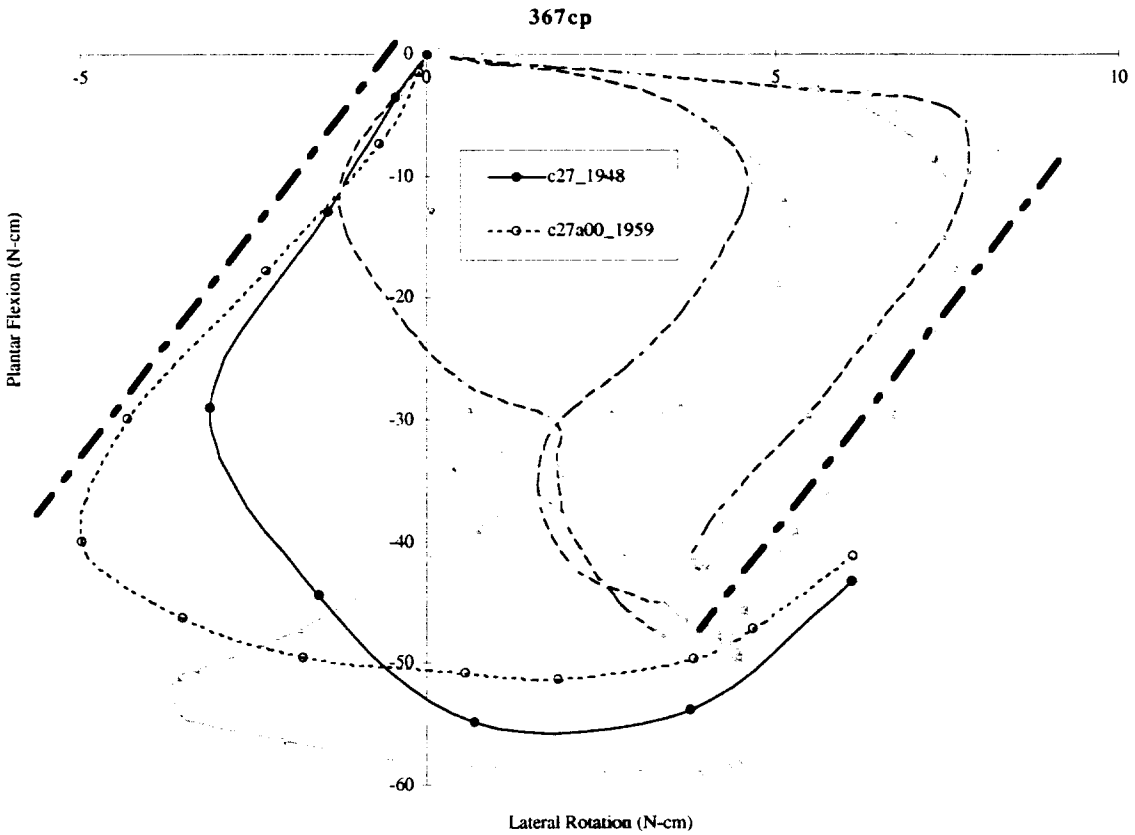

Figure C.3 – This figure illustrates the torque traces produced using the 270° contact alone (circles with black line, c27_1948). Anodic steering current from the 0° contact was added to monopolar current at the 270° position (open circles with dashed line, c27a00_1959). The torque output produced by these two currents can be compared by stimulating different contacts on the common peroneal branch (gray lines). The number after the underscore (_) in each label is the time (on a 24hr clock) at which the data were collected.

Experiment #4: Cat #387

In the fourth experiment, cat #387, sub-fascicular separation was achieved by using the electrodes on the tibial nerve, Figure C.4. Plantar flexion torque representative of the PLN were produced first using the #1 contact on the tibial cuff while the #4 contact on the tibial cuff produced medial rotation representative of the FHL/FDL/TP first. Stimulation from the 180° position was able to achieve the tibial nerve, shown in Figure C.4. Anodic and cathodic steering currents were added from the 90° contact (c18a09_1845 anodic steering, c09c18_1615 cathodic steering) and the 270° contact (c18a27_1901 anodic steering, c18c27_1647 cathodic steering). In each of the attempted cases, the steering current was fixed at a single value, 90% of threshold. In no case were we able to effect the desired separation between FHL/FDL/TP and PLN. It is possible that a better level of separation could have been possible if more than one level of steering had been used.

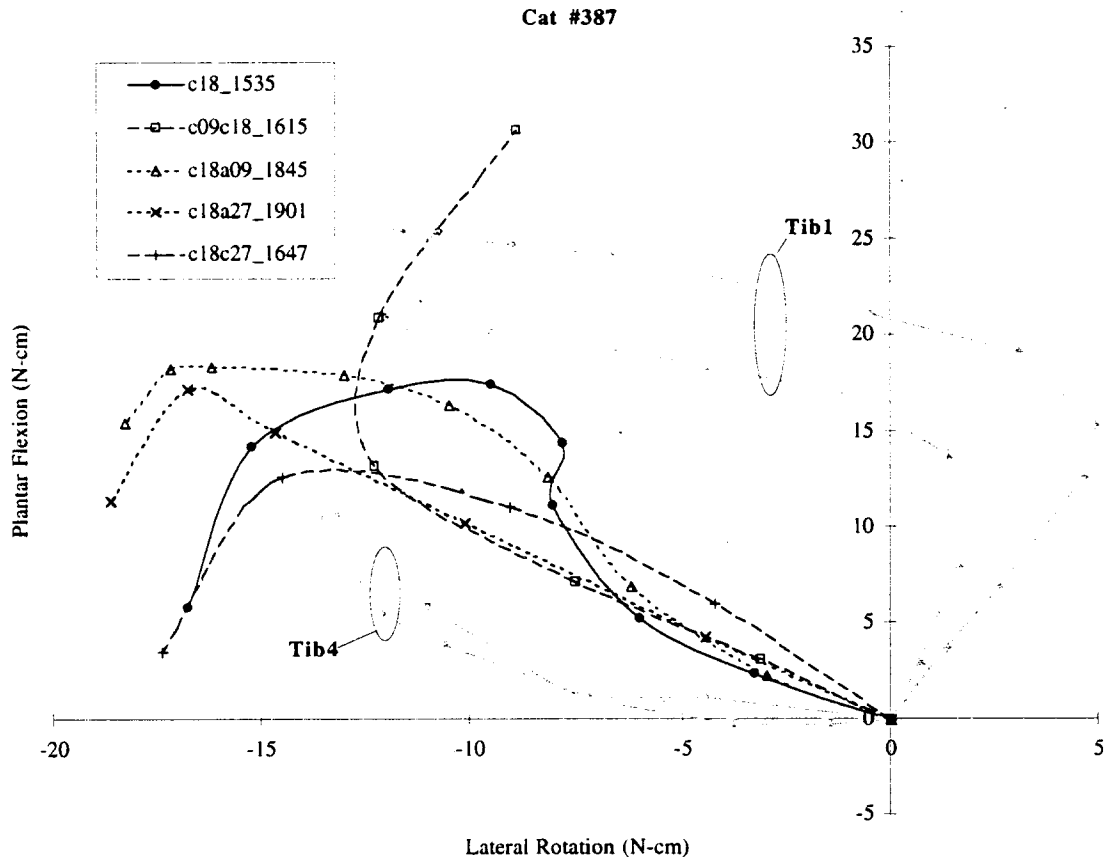

Figure C.4 – This figure displays the torque traces produced using the 180° contact (c18_1535) as a monopole. When anodic or cathodic steering current was added it was compared to the torque output produced by stimulating different contacts on the common peroneal branch (gray lines). Anodic and cathodic steering currents were added from the 90° contact (c18a09_1845 anodic steering, c09c18_1615 cathodic steering) and the 270° contact (c18a27_1901 anodic steering, c18c27_1647 cathodic steering). The number after the underscore (_) in each label is the time (on a 24hr clock) at which the data were collected.

Conclusion

Although the results of these four experiments are not conclusive, these results suggest that sub-fascicular separation is possible using steering current techniques. These results are also not exhaustive and we believe that improvements in stimulator control and additional stimulation paradigms, including the cathodic pre-pulse, could be used to achieve additional selectivity of the sub-fascicular axon populations. These results, however, indicate that selective activation of the nearest or most excitable axon population within in the fascicle does occur in some cases. At present, attempts to refine the pre-pulse technique are being conducted in order to use this technique to excite the more distant or less excitable populations within the fascicle before the closer or more excitable populations.

C.I.2.3: Continuous torque space

Abstract

Activation of multiple muscles at different levels of activation has produced torque outputs that indicate all points in the physiologically defined torque space can be achieved. In the use of a motor prosthesis, multiple select muscles need to be simultaneously activated. Using a nerve cuff electrode, select regions of a nerve trunk serving individual muscles or muscle groups can be activated. Activation of multiple muscles can be achieved by using either a field steering approach to shift the activated region between different muscles, or by using two different contacts stimulated with a short delay between the pulses. This delay is in order to avoid field effects from the combination of pulses. Field Steering was used in four animals to achieve a range of torque outputs. Using the field steering output, torque vectors representing the entire space of possible outputs in a particular region or of the entire usable space were achieved. Using the time difference technique we believe will be an important technique and will be tested in both acute and chronic animal studies.

Purpose

The purpose of this project is to demonstrate that a motor nerve serving multiple muscles can be activated at various levels to produce the full range of torque outputs possible. The model system studied uses a four contact self-sizing cuff electrode placed on the cat sciatic nerve, which contains four major branches that serve the 13 muscles controlling the torque produced about the ankle. The focus of the studies reported here was to first show separate and distinct motor axon populations within either the common peroneal or tibial nerves. The objective was to then demonstrate that these distinct motor axon populations, serving separate muscles, could be activated separately and independently with "field steering" and/or "pre-pulse" techniques.

Background

In order to restore function to spinal cord injured patients, motor prostheses simultaneously activate multiple muscles to different levels of activation. Present motor prostheses require an electrode for every muscle to be stimulated. Using a nerve cuff electrode, a single electrode array can control all of the muscles controlling a joint. Previous studies have shown that select regions of a nerve trunk serving individual muscles or muscle groups can be activated using a nerve cuff electrode. Torque outputs that are the result of the sum of multiple muscles can be achieved by using either field steering techniques to shift the activated region between regions of axons serving different muscles. These outputs can also be achieved by using two different contacts stimulated with pulses having a short delay between the pulses to avoid field effects from the combination of pulses.

Experiment #1: Cat #302

These data were first presented in QPR#4 to illustrate that steering current could be varied to multiple levels. Shown in Figure C.5 is the torque evoked around the ankle joint of Cat #302. In this animal, the region between the negative lateral rotation axis and half way to the negative plantar flexion axis, about 45°, was achieved by using steering currents. Steering currents were used to smoothly and gradually change the excitatory field of the 270° contact to activate selectively the common peroneal branch. The application of cathodic stimuli of varying

amplitudes to contact 270° alone was found to produce medial rotation as shown in Figure C.5 by the square and triangle data points connected by a gray line. The length of the horizontal line extending from each datum point is proportional to the amount of longitudinal current applied to achieve that output torque. The torque output produced by the application of cathodic stimuli of varying amplitudes to the common peroneal branch at three different times during the experiment is shown in the gray circles, squares, and triangles clustered near the dorsiflexion axis. The remaining data were achieved through the simultaneous application of cathodic stimuli of varying amplitudes to contact 270° and an anodic stimuli of varying amplitudes between contact 180° returning through contact 270°. The combination of stimuli produced a range of torque that encompassed the region of torque space between the torque output produced by activation of the 270° contact alone and that produced by the common peroneal branch alone. Each datum point from the combined stimulation has a line composed of a horizontal component, which is proportional to the current applied to the 270° contact, and a vertical component, which is proportional to the anodic steering current applied to the 180° contact. These vector lines indicate that an increase in the steering current and a decrease in the longitudinal contact current steers the excitatory field in the direction of the common peroneal fascicle within the nerve trunk.

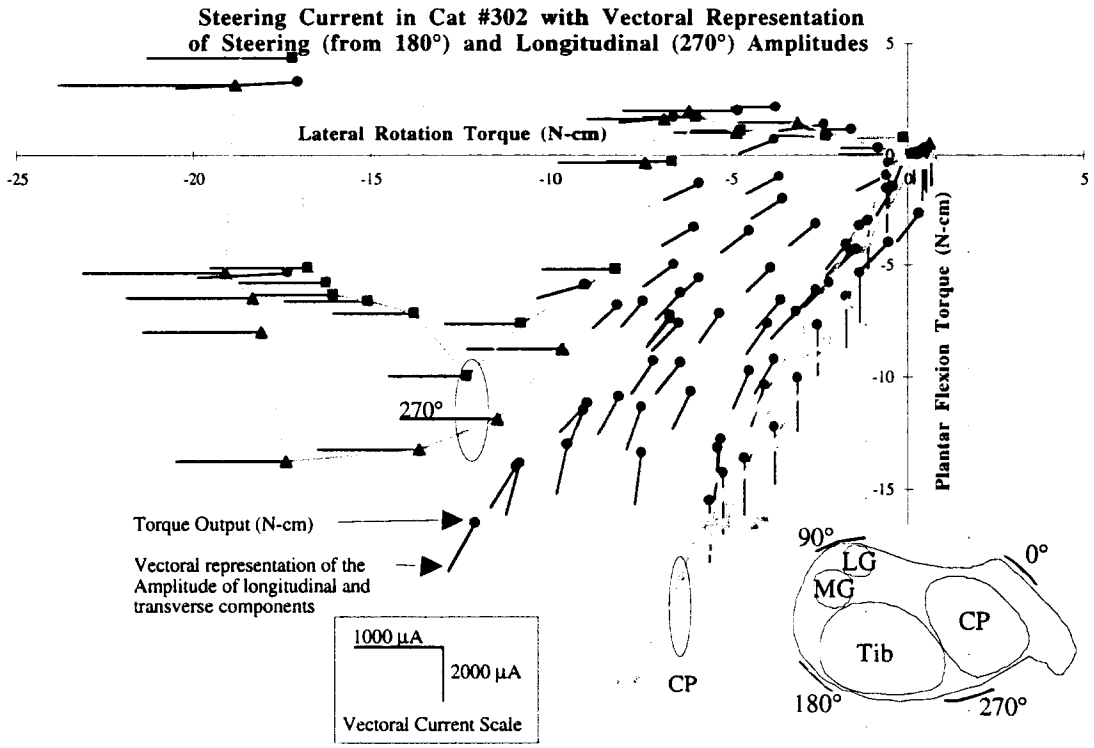

Figure C.5 - Torque output produced using the 270° contact with anodic steering current applied to the 180° contact. The gray lines indicate the torque output resulting from direct stimulation of the common peroneal (close to the negative y-axis) or from stimulating the 270° contact in a monopolar configuration (along the negative x-axis). The vector line extending from each datum point represents both the amount of longitudinal current that was applied to the 270° contact by the x component of the vector, and the amount of steering current that was applied between the 180° contact and the 270° contact by the y component of the vector.

Experiment #2: Cat #367

In Figure C.6 is shown the data collected when steering currents were applied to the 0° contact in cat #367. Anodic steering from the 90° contact applied to the 0° contact is shown with the open circle data points while anodic steering from the 270° contact applied to the 0° contact is shown with the "+" data points. Close to the origin, all of the data recorded were in a single line corresponding to the torque output of the LG, shown in gray. These data illustrate that steering currents can be used to achieve any point between the x-axis and about the 45° angle. The algorithm used to collect these data was too time consuming and was therefore modified for future experiments.

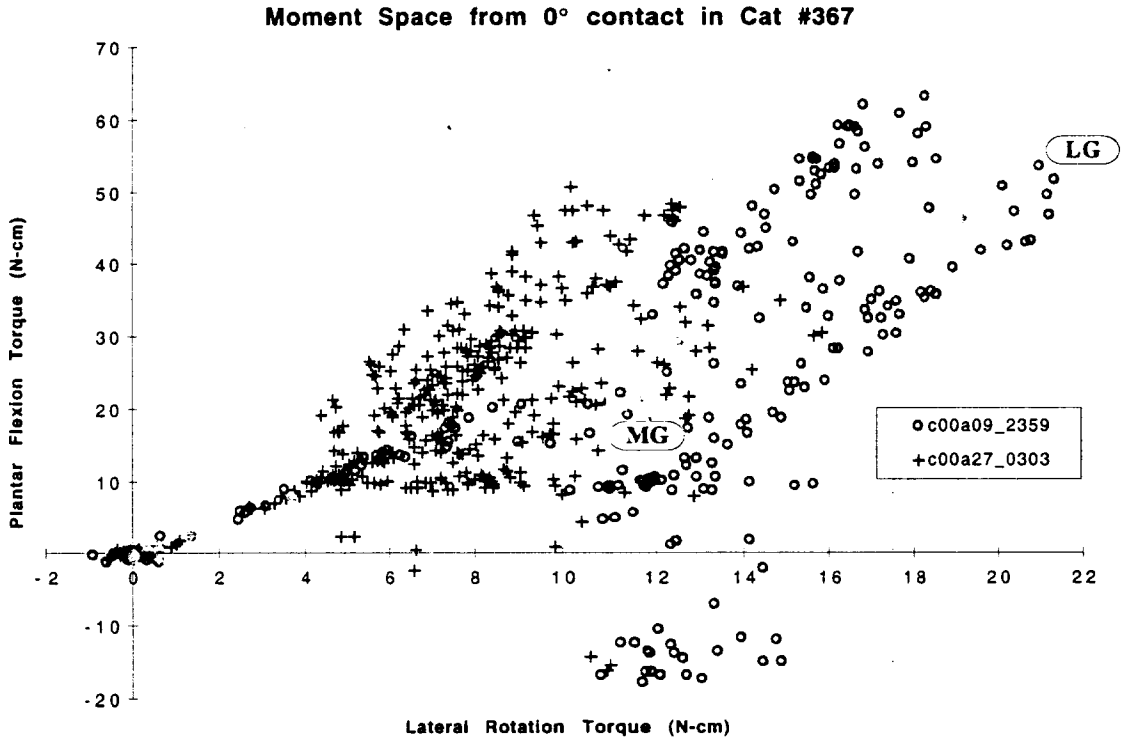

Figure C.6 - Torque output produced using the 0° contact with anodic steering current applied to either the 90° contact, shown by the open circles, or the 270° contact, shown by the plus signs.

Experiment #3: Cat #387

In Figure C.7 is shown the data collected during an experiment on cat #387. The gray lines show the torque output when stimuli were applied to each of the individual branches. The dark lines were the torque output when stimuli were applied to each of the contacts of the electrode when stimulated as a monopole. The remaining points on the graph represent the following: the torque output achieved using cathodic steering from the 0° and 180° contacts together ("x" data points), the 90° and 180° contacts together ("o" data points), the 90° and 270° contacts together ("Δ" data points), and the 180° and 270° contacts together ("+" data points). The fact that data points are scattered over much of the entire moment space suggests that it will be possible to achieve all points in torque space by some combination of stimulus parameters.

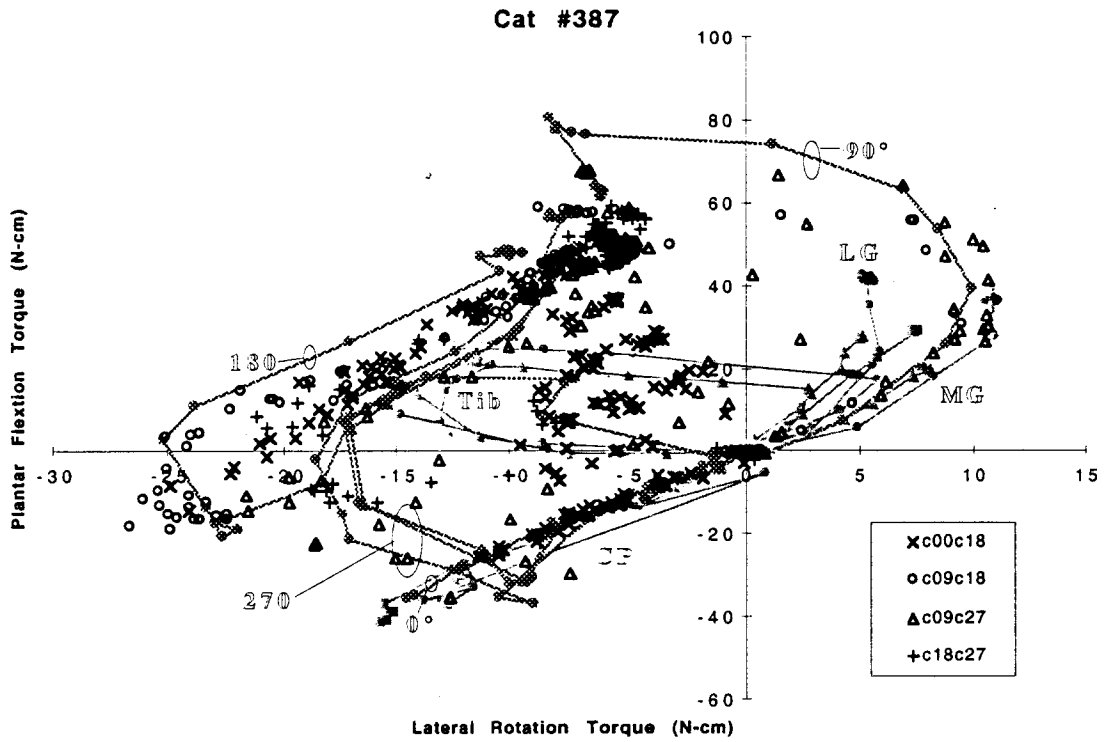

Figure C.7 - Torque output produced using the cathodic steering current applied to a combination of different contacts. Cathodic steering current applied to the 0° and 180° contacts together is shown by the 'x' data points. Cathodic steering current applied to the 90° and 180° contacts together is shown by the 'o' data points. Cathodic steering current applied to the 90° and 270° contacts together is shown by the 'Δ' data points. Cathodic steering current applied to the 180° and 270° contacts together is shown by the '+' data points.

Conclusions

Field Steering techniques were used in four animals to achieve a torque output that covers a wide range of the physiologically possible points in ankle torque space. The results are encouraging and support the hypothesis that self-sizing multicontact cuff electrodes can be used to effect selective and independent control of motor nerves (e.g. the motor nerves serving the thirteen major muscles acting on the ankle joint) that are collected together in a single large nerve (e.g. the sciatic nerve). These studies will be continued in the next reporting period.

REFERENCES

Brushart, T.M.E. "Central Course of Digital Axons Within the Median Nerve of Macaca Mulatta." J Comp Neur, 311:197-209 (1991).

Grill, W.M., and J.T. Mortimer. "Non-invasive measurement of the input output properties of peripheral nerve stimulating electrodes." J Neurosci Methods, 65:43-50 (1996).

Hallin, R.G. "Microneurography in relation to intraneural topography: somatotopic organization of median nerve fascicles in humans." J Neurol Neurosurg Psychiatry, 53:736-744 (1990).

J. H. Lawrence, T. R. Nichols, and A. W. English, "Cat Hindlimb Muscles Exert Substantial Torques Outside the Sagittal Plane," *J Neurophys*, vol. 69, pp. 282-285, 1993.

Schady, W., J.L. Ochoa, H.E. Torebjork, and L.S. Chen. "Peripheral Projections of Fascicles in the Human Median Nerve." Brain, 106:745-760 (1983).